Proceedings of IMECE'05
2005 ASME International Mechanical Engineering Congress & Exposition
Orlando, Florida, November 5-11, 2005

IMECE2005-81525

A SCREW-THEORETIC ANALYSIS FRAMEWORK FOR PAYLOAD MANIPULATION BY MOBILE MANIPULATOR COLLECTIVES

Rajankumar Bhatt
Mechanical & Aerospace Engineering
State University of New York at Buffalo
318 Jarvis Hall, Buffalo NY 14260 USA
E-mail: rmbhatt@eng.buffalo.edu

Chin Pei Tang
Mechanical & Aerospace Engineering
State University of New York at Buffalo
318 Jarvis Hall, Buffalo NY 14260 USA
E-mail: chintang@eng.buffalo.edu

Michel Abou-Samah
Application Engineer
MSC Software Corporation
E-mail: gishm@hotmail.com

Venkat Krovi
Mechanical & Aerospace Engineering
State University of New York at Buffalo
318 Jarvis Hall, Buffalo NY 14260 USA
E-mail: vkrovi@eng.buffalo.edu

ABSTRACT

In recent times, there has been considerable interest in creating and deploying modular cooperating collectives of robots. Interest in such cooperative systems typically arises when certain tasks are either too complex to be performed by a single agent or when there are distinct benefits that accrue by cooperation of many simple robotic modules. However, the nature of the both the individual modules as well as their interactions can affect the overall system performance.

In this paper, we examine this aspect in the context of cooperative payload transport by robot collectives wherein the physical nature of the interactions between the various modules creates a tight coupling within the system. We leverage the rich theoretical background of analysis of constrained mechanical systems to provide a systematic framework for formulation and evaluation of system-level performance on the basis of the individual-module characteristics.

The composite multi-d.o.f wheeled vehicle, formed by supporting a common payload on the end-effectors of multiple individual mobile manipulator modules, is treated as an in-parallel system with articulated serial-chain arms. The system-level model, constructed from the twist- and wrench-based models of the attached serial chains, can then be systematically analyzed for performance (in terms of mobility and disturbance rejection.) A 2-module composite system example is used through the paper to highlight various aspects of the systematic system model formulation, effects of selection of the actuation at the articulations (active, passive or locked) on system performance and experimental validation on a hardware prototype test bed.

I. INTRODUCTION

Biologists who study animal aggregations such as swarms, flocks, school and herds have observed the remarkable group-level cooperative achievement of tasks. For example, armies of ants leverage the collective strength and manipulation capabilities to move large food-pieces, which would be impossible for a single ant. Thus, there is a considerable interest in engineering such teams/collectives of land-based mobile agents to achieve common goals in various application arenas from collective foraging to cooperative payload transport.

On one hand, deploying such teams of smaller, simpler robot modules can yield significant benefits over deploying a single larger robot in terms of redundancy, robustness and reliability. Other important benefits include capability for decentralization, as well as ability to reconfigure to improve performance. On the other hand, such modularity creates challenges by way of increased choice, in terms of the number of possible ways to accomplish a given task. In particular, in a modularly composed system, both the nature of the *individual modules* as well as their *interactions* can affect the overall system performance. Hence, a systematic (and preferably quantitative) framework for evaluation of the individual module- and system-level characteristics is desirable and remains one of the underlying goals of our research efforts. This is an aspect that we examine in the context of cooperative payload transport by robot collectives in this paper.

Many of the entailed issues are highlighted in the illustrative example of household furniture movers moving a large piece of furniture. Traditionally, such movers employ variable numbers of modular wheeled dollies, as determined by the payload. These are positioned at suitable locations to ensure mobility, stability and load-distribution within the aggregation, which is then steered away as a single composite system. Occasionally, additional dollies may be added or the relative locations of existing dollies may be readjusted to avoid obstacles or to enhance overall performance. Thus, a fleet of semi-autonomous wheeled modules that can cooperate to either assist the human operator or autonomously perform this overall payload transport process would have tremendous application in many material handling situations.

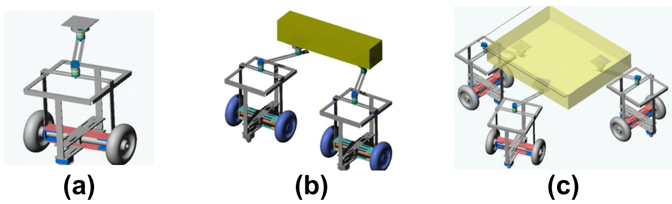

Figure 1: (a) An individual mobile manipulator module, and a composite system formed by (b) 2 modules, and (c) 3 modules.

All our individual modules take the form of differentially-driven Wheeled Mobile Robots (WMR) with a mounted manipulator arm, as shown in Figure 1(a). A composite multi-d.o.f. wheeled vehicle is formed when a payload is placed at the end-effectors of multiple such modules. However, two or more wheeled mobile robots, with rigid axles, cannot be arbitrarily coupled to each other due to the incompatibility of the velocities of the wheels. The potential degradation in the overall performance can range from loss of mobility, rattle-shake, unintentional compliance, wear and tear of the tires and wheel slip. Hence, many approaches in the literature [1, 2] advocate the addition of further articulations between the various wheels/axles in order to accommodate the rigid body constraints – in our system this role is played by the mounted planar manipulator arm. The resulting composite vehicle, of the form shown in Figure 1(b)-(c), possesses: (i) ability to accommodate changes in the relative configuration (by virtue of the compliant linkage); (ii) a mechanism for detecting such changes (using sensed articulations); and (iii) means to compensate for such disturbances (using the redundant actuation of the bases), while performing the payload transport task.

In general, a careful selection of the type, number, dimensions and actuation of both the wheels attached to the base and the joints in the mounted manipulator are critical to determining the performance of the individual module. However, these aspects are examined elsewhere [3, 4], and yield the mobile manipulator configuration design shown in Figure 1(a). Using this base module, it is our desire to create a composite vehicle that can be analyzed for performance in terms of mobility and disturbance rejection. In particular, we wish to address the following questions: i) Can the system *accommodate* arbitrary end-effector motions?; (ii) Can the system *create* arbitrary end-effector motions?; (iii) Can the system *resist* arbitrary end-effector forces?; (iv) What effect do various actuation schema have on system performance?

To this end, we leverage the rich history and background of analysis methods for constrained articulated mechanical systems. In particular, a twist- and wrench-based analysis of in-parallel systems created with the articulated serial-chain legs/arms provides the underlying framework for examining the performance of the cooperative system in our paper. The unique contribution of this paper comes from: the systematic modeling of the novel nonholonomic wheeled mobile manipulators (which form the serial-chain arms/legs); the systematic formulation of the in-parallel composite system model and subsequent analysis of the effects of selection of the actuation at the articulations (active, passive or locked) on system performance.

The rest of the paper is organized as follows: Section II presents a brief overview of the pertinent literature. Twist-based modeling of the wheeled mobile manipulator module is introduced in Section III. In Section IV, the wrench system of the single mobile manipulator is determined with different actuation schemes. Section V analyzes different cases of collaboration of such two modules, followed by the experimental results. Section VI concludes the paper with some discussions.

II. BACKGROUND

Cooperative multi-robot systems, ranging from multiple mobile robots [5, 6], multiple manipulators [7], multi-fingered hands [8, 9] and multi-legged vehicles [10, 11] have been extensively studied in a variety of contexts. We will restrict our attention to cooperative physical manipulation by articulated wheeled mobile manipulators [12-16] focusing on the motion and force distribution issues.

Khatib et al. [12] develop a decentralized control structure for cooperative tasks with mobile manipulation systems with holonomic bases and fully actuated manipulators. Motion planning has also been considered for collaborating teams of nonholonomic mobile manipulators from various centralized perspectives [13, 14]. Kosuge et al. [15] propose a simple method for carrying a large object by cooperation of multiple mobile manipulators with impedance based controllers by selectively locking and unlocking some joints of the mounted manipulators on mobile platforms. Yamakita et al. [16] implement the Passive Velocity Field Control approach for the cooperative control of multiple mobile robots holding an object. In almost all these cases, the principal emphasis is on control of a system formed with generic wheeled mobile manipulator modules. Despite the significant influence on the overall system performance, typically scant attention is paid either the nature of the module (type, dimensions or actuation of the wheels and/or the articulations), a shortcoming that we will address in this paper.

On a slightly different note, we also see that the composite system formed by connecting the multiple mobile manipulators to the common payload share many features with the class of Multi-Degree-of-Freedom (MDOF) Wheeled Vehicles [1, 17-22]. While some of these like the RollerRacer [17] and the Snakeboard [18] are case-studies in underactuated locomotion, several others like OMNIMATE/CLAPPER [1] and systems with multiple actively steered wheels [19-21] and WAAVs [22] feature redundancy in actuation. Several of these authors also note that despite gains in maneuverability over conventional mobile robots, the overconstrained nature with hybrid series-parallel kinematic chains creates challenges in design, planning and control of such systems. The twist- and wrench-based analysis methods adopted in this paper offer convenient tools for systematic system-level motion- and force-analysis based on the capabilities of the individual modules.

III. TWIST MODELING OF A SINGLE MOBILE MANIPULATOR MODULE

We briefly summarize the mathematical preliminaries required in the twist (velocity) level formulation. The reader is referred to [23-25] for greater details.

In a two-dimensional Euclidean task space, the configuration of a rigid body can be represented as an element $A \in SE(2)$. In our notation, the relative configuration of a moving frame $\{E\}$ relative to a fixed frame $\{F\}$ is defined by the homogeneous transformation in a 3×3 matrix of

$$ {}^F A_E = \begin{bmatrix} {}^F R_E & {}^F \underset{\sim}{d} \\ \underset{\sim}{0}^T & 1 \end{bmatrix} \tag{1} $$

where ${}^F R_E \in SO(2)$ is a rotation matrix, and ${}^F \underset{\sim}{d} \in \mathbb{R}^2$ is a displacement vector. In planar case, a twist matrix $T \in se(2)$ can be represented by a 3×3 matrix of the form

$$ T = \begin{bmatrix} \Omega & \underset{\sim}{v} \\ \underset{\sim}{0}^T & 0 \end{bmatrix} \tag{2} $$

where $\Omega = \begin{bmatrix} 0 & -\omega \\ \omega & 0 \end{bmatrix} \in so(2)$ is a skew-symmetric matrix, $\omega \in \mathbb{R}$, and $\underset{\sim}{v} \in \mathbb{R}^2$. The twist vector then takes the form of $\underset{\sim}{t} = \begin{bmatrix} \omega \\ \underset{\sim}{v} \end{bmatrix} \in \mathbb{R}^3$. Note that ω is an angular velocity scalar and $\underset{\sim}{v}$ is a linear velocity vector in the plane. In our context, a body-fixed twist matrix corresponding to the motion of the moving frame $\{E\}$ with respect to its immediately preceding frame $\{F\}$ (as expressed in frame $\{E\}$) can be formed by

$$ {}^E\left[{}^F T_E\right] = {}^F A_E^{-1}\, {}^F \dot{A}_E \tag{3} $$

Such motion description expression is particularly useful in the study of locomotion systems since it is invariant to the changes with respect to the inertial-fixed frame. The twist matrix can then be transformed to any arbitrary frame $\{N\}$ by a similarity transformation of

$$ {}^N\left[{}^F T_E\right] = \left[{}^N A_E\right] {}^E\left[{}^F T_E\right] \left[{}^N A_E\right]^{-1} \tag{4} $$

Figure 2 depicts a differentially-driven WMRs with a 2R manipulator mounted at the midpoint of the wheel axle and denoted as an NH-RR type mobile manipulator. The frame $\{M\}$ is rigidly attached to center of the WMR with the X_M-axis oriented in the direction of the forward travel of the mobile robot, and Y_M-axis oriented at direction perpendicular to X_M-axis, i.e. the direction of the nonholonomic constraint. Frame $\{E\}$ is attached to the frame of reference of the payload, as depicted in Figure 2(a). Thus, the second link is a "virtual link" that connects from the point of attachment of the manipulator with the payload to the payload reference frame. The configuration of the manipulator with the two revolute joints can be parameterized by the two relative angles θ_1 and θ_2, with the link lengths L_1 and L_2. The frame $\{A\}$ is rigidly attached at the distal end of the first link.

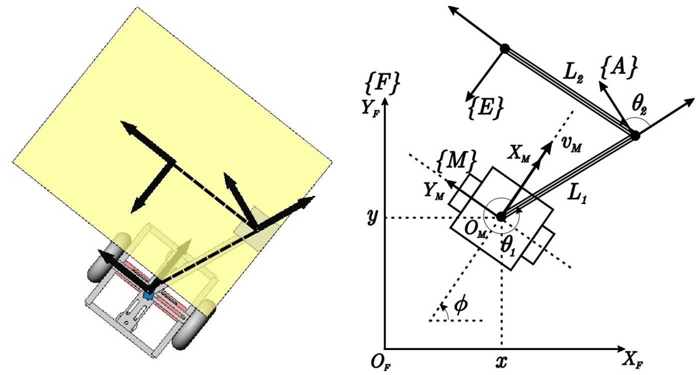

Figure 2: A nonholonomic mobile manipulator (NH-RR) module (a) a CAD model and (b) the corresponding schematic.

The kinematic model of the mobile manipulator is developed by composition of contributions from the mobile platform and the manipulator. In the final form, we would like to express all the twist vectors in the payload reference frame $\{E\}$. The twist of the mobile platform expressed in frame $\{M\}$, *including the effect of nonholonomic constraints*, can be written as:

$$ {}^M\left[{}^F T_M\right] = {}^M\begin{bmatrix} 0 & 1 & 0 \\ -1 & 0 & 0 \\ 0 & 0 & 0 \end{bmatrix} \dot{\phi} + {}^M\begin{bmatrix} 0 & 0 & 1 \\ 0 & 0 & 0 \\ 0 & 0 & 0 \end{bmatrix} v_M \tag{5} $$

where $\dot{\phi}$ and v_M are the angular and linear forward velocities of the mobile platform, respectively. The twists in Eq. (5) can be expressed in frame $\{E\}$ by the similarity transformation in Eq. (4). The total manipulator twist can be expressed as a linear combination of the twist matrices of each d.o.f in the form of:

$$ {}^E\left[{}^M T_E\right] = {}^E\left[{}^M T_A\right]\dot{\theta}_1 + {}^E\left[{}^A T_E\right]\dot{\theta}_2 \tag{6} $$

The Jacobian matrix of the combined system can be expressed as:

$$ {}^E\left[{}^F \underset{\sim}{t}_E\right] = \begin{bmatrix} | & | & | & | \\ \underset{\sim}{t}_1 & \underset{\sim}{t}_2 & \underset{\sim}{t}_3 & \underset{\sim}{t}_4 \\ | & | & | & | \end{bmatrix} \begin{bmatrix} \dot{\phi} \\ v_M \\ \dot{\theta}_1 \\ \dot{\theta}_2 \end{bmatrix} \tag{7} $$

where

$$ \underset{\sim}{t}_1 = \begin{bmatrix} 1 \\ L_1 S_2 \\ L_1 C_2 + L_2 \end{bmatrix},\ \underset{\sim}{t}_2 = \begin{bmatrix} 0 \\ C_{12} \\ -S_{12} \end{bmatrix},\ \underset{\sim}{t}_3 = \begin{bmatrix} 1 \\ L_1 S_2 \\ L_1 C_2 + L_2 \end{bmatrix},\ \underset{\sim}{t}_4 = \begin{bmatrix} 1 \\ 0 \\ L_2 \end{bmatrix} $$

and $S_{ab\cdots} = \sin(\theta_a + \theta_b + \cdots)$ and $C_{ab\cdots} = \cos(\theta_a + \theta_b + \cdots)$.

The columns of this Jacobian matrix correspond to the vector-fields spanning the distribution of feasible twists. For the remainder of the paper, we will denote the end-effector twist ${}^{E}\underset{\sim}{t}$ instead of ${}^{E}\left[{}^{F}\underset{\sim}{t}_E\right]$. We can separate the Jacobian matrix into submatrices of $\left[J_a\right]$ (active Jacobian matrix) and $\left[J_p\right]$ (passive Jacobian matrix), where they are formed by the active and passive twist vectors, respectively. Locked joints do not contribute to the end-effector twist and are not included in any of the Jacobian matrix. Semi-active (spring-loaded) joints can be treated as locked joints if the developed torque at the joint is less than the preload, or as passive if developed torque is more than the preload. The articulated linkage is able to create an arbitrary end-effector twist ${}^{E}\underset{\sim}{t}$ if it falls in the span of the active distribution. If an arbitrary twist ${}^{E}\underset{\sim}{t}$ is spanned by the passive distribution, the articulated linkage can accommodate this disturbance. For further details of such twist analysis, see [26].

IV. WRENCH MODELING OF A SINGLE MOBILE MANIPULATOR MODULE

The wrench system at the end-effector of each mobile manipulator module can be systematically developed on the basis of reciprocity relationships. Corresponding to each planar twist $\underset{\sim}{t}_k$, we can determine a wrench W_k such that it is reciprocal to all other twists in the chain, except the k^{th} twist. Mathematically, this can be denoted as:

$$\left[W_k\right] \circ \underset{\sim}{t}_j = 0, \text{ for } j \neq k \tag{8}$$

W_k represents the instantaneous wrench that can be sustained by the linkage when joint k is actuated and is called *Selectively Non-Reciprocal Screw* (SNRS) [27]. Wrench W_k is an element of the dual vector space to the space of twist that takes the form of $\begin{bmatrix} F_x & F_y & M_z \end{bmatrix}^T \in \mathbb{R}^3$. A set of such wrenches is created at the end-effector by considering all actuated joints within the serial chain. The span of all such wrenches now determines the total wrench $\underset{\sim}{F}$ that can be applied or actively equilibrated and is represented as:

$$\underset{\sim}{F} = \sum_{k=1}^{N_a} W_k w_k = [W]\underset{\sim}{w} \tag{9}$$

where N_a is the number of actuated joints, w_k is the wrench intensity of the k^{th} actuated joint.

In our work, we also wish to consider the role of different actuation schemes and denote active joints as A, passive joints as P, and locked joints as L. For each NH-RR module, we may denote the overall actuation scheme by a triple. The first alphabet corresponds to the actuation of the nonholonomic base, second and third alphabets represent the actuation of the first (θ_1) and second (θ_2) joints of the manipulator. For instance, A-LP represents the module with nonholonomic base active, first joint held locked but second joint held passive. In the rest of this section, we will briefly develop the instantaneous wrenches corresponding to each joint for two particular modules: (a) A-PP and (b) A-LP. Other possibilities are presented in Appendix A.

Case A: A-PP Module

For an A-PP module, the end-effector twist depends on all four twists of the full Jacobian matrix as:

$$ {}^{E}\underset{\sim}{t} = \begin{bmatrix} | & | & | & | \\ \underset{\sim}{t}_1 & \underset{\sim}{t}_2 & \underset{\sim}{t}_3 & \underset{\sim}{t}_4 \\ | & | & | & | \end{bmatrix} \begin{bmatrix} \dot{\phi} \\ v_M \\ \dot{\theta}_1 \\ \dot{\theta}_2 \end{bmatrix} \tag{10}$$

Hence, the instantaneous selectively non-reciprocal wrench system can be determined as:

$$W_1 = \varnothing, W_2 = \begin{bmatrix} -\dfrac{C_2}{S_2} \\ 1 \\ -L_2 \end{bmatrix}, W_3 = \varnothing, W_4 = \begin{bmatrix} \dfrac{S_{12}}{C_{12}} \\ 1 \\ \dfrac{-L_1 C_1}{C_{12}} - L_2 \end{bmatrix} \tag{11}$$

where $\varnothing$ is a null set. Each of these wrenches also has a geometric interpretation as lines of action of forces as expressed in the end-effector frame (see W_2 and W_4 in Figure 3).

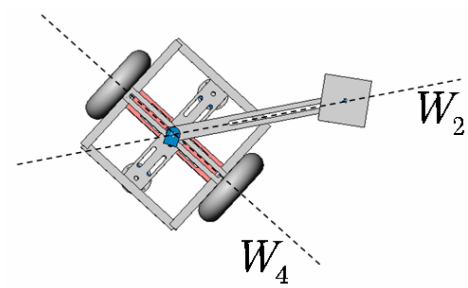

Figure 3: Lines of action of wrench of single mobile manipulator module for Case A – A-PP Module

Case B: A-LP Module

We have to consider the case of locked joints specifically since the twist contribution of the locked joint now gets eliminated from the total Jacobian matrix. For an A-LP module, the total twist becomes:

$$ {}^{E}\underset{\sim}{t} = \begin{bmatrix} | & | & | \\ \underset{\sim}{t}_1 & \underset{\sim}{t}_2 & \underset{\sim}{t}_4 \\ | & | & | \end{bmatrix} \begin{bmatrix} \dot{\phi} \\ v_M \\ \dot{\theta}_2 \end{bmatrix} \tag{12}$$

Thus, the instantaneous selectively non-reciprocal wrenches of this case are:

$$W_1 = \begin{bmatrix} \dfrac{S_{12}}{C_{12}} \\ 1 \\ -L_2 \end{bmatrix}, \; W_2 = \begin{bmatrix} -\dfrac{C_2}{S_2} \\ 1 \\ -L_2 \end{bmatrix}, \; W_4 = \begin{bmatrix} \dfrac{S_{12}}{C_{12}} \\ 1 \\ \dfrac{-L_1 C_1}{C_{12}} - L_2 \end{bmatrix} \tag{13}$$

Figure 4 depicts the lines of actions of the wrenches W_1, W_2, W_4 for an A-LP module. Similarly, the selected nature of actuation (A, P or L) of the two joints of the manipulator arm creates many cases.

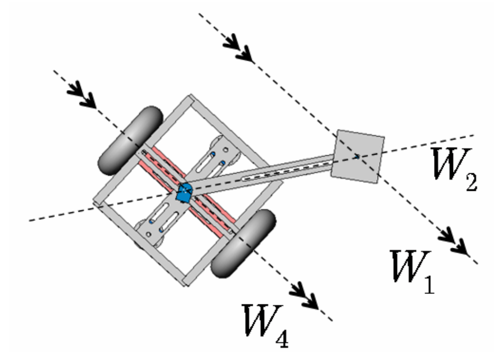

Figure 4: Lines of action of wrench of single mobile manipulator module for Case B – A-LP Module

V. COOPERATIVE SYSTEM ANALYSIS

In this section, we consider the collaboration between *two* NH-RR type mobile manipulator modules carrying a common payload. The end-effectors of the physical manipulators are assumed to be rigidly attached to the payload and that we are given apriori, the locations of the attachments of these fixture sites, with respect to the object reference frame. We also consider a frame attached to a point of interest on the common payload as the end-effector frame of both the flanking mobile manipulator systems (see Figure 5). In doing so, the individual modules may be treated as the serial chains legs/arms of an in-parallel mechanism.

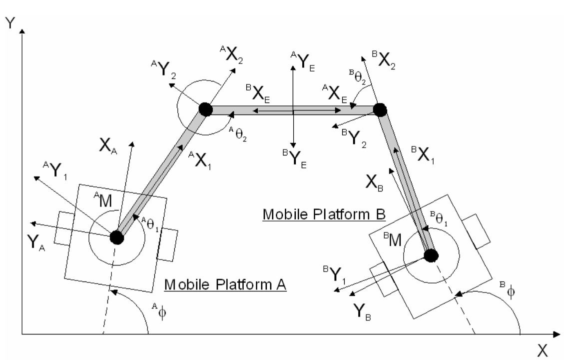

(a)

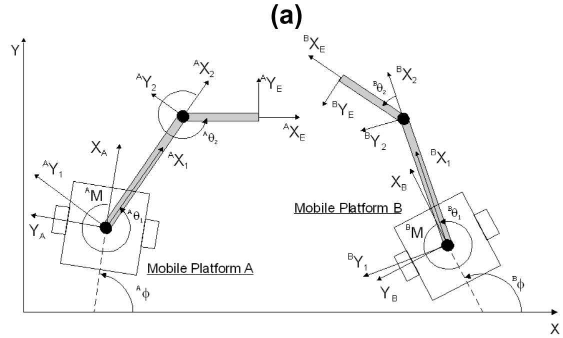

(b)

Figure 5: Overall system considered as: (a) composite system; or (b) independent mobile manipulators.

System Twist Analysis

In all cases where the composite system is considered as the mobility of the system, i.e. ability to accommodate arbitrary twist disturbance or create arbitrary end-effector twist is completely characterized by examining the twists within each sub-chain as we showed in [26].

System Wrench Analysis

However, in order to analyze the force capabilities of the system, we need to also consider the contributions from the other modules arising from the series-parallel duality of the in-parallel system [28]. We now also study the effect of selection of actuation on the performance of the composite system.

For a parallel mechanism, when N_b different branches lead to the same end-effector forming a closed chain, the resultant wrench $\underset{\sim}{F}_p$ must lie in the span of the end-effector wrenches due to the individual branches. Let $\underset{\sim}{W}_k^i$ be the instantaneous wrench applied by the branch i when the k^{th} joint is actuated. Thus,

$$\underset{\sim}{F}_p = [\mathbf{W}]\,\underset{\sim}{w} \tag{14}$$

where $[\mathbf{W}] = \text{column}\left(W_k^{\ i}\right)$, for $k = 1,....,N$ (number of active d.o.f. within the i^{th} branch) and $i = 1,....,N_b$ (number of branches) and $\underset{\sim}{w}$ is the vector of corresponding wrench intensities. For non-redundant actuation, $[\mathbf{W}]$ is a square matrix and if it is nonsingular, the unknown vector of resultant forces can be calculated as

$$\underset{\sim}{w} = [\mathbf{W}]^{-1}\,\underset{\sim}{F}_p \tag{15}$$

However, if $[\mathbf{W}]$ is singular, the forces from each branch do not the span force system that is required to apply or sustain at the end-effector. Thus, such parallel mechanism is *force unconstrained*. For a redundant system, $[\mathbf{W}]$ is generally a non-square matrix that is not invertible. In such case, a set of square matrices can be constructed by considering each combination of columns that can create a square matrix, and those conditions that satisfy the singularity for each such sub-matrix are the singularity condition for the system [29].

Case A: Cooperation between A-PP and A-PP

To begin with, we consider the case of two A-PP modules, i.e. the articulations on both mounted manipulators are passive. Let ${}^{A}\Gamma_w$ denote the adjoint wrench transform [23] from frame $\left\{{}^{B}X_E,\ {}^{B}Y_E\right\}$ to frame $\left\{{}^{A}X_E,\ {}^{A}Y_E\right\}$, i.e. the preferred payload frame (see Figure 5). The combined wrench system, in this case, can be written as

$$\begin{bmatrix} | & | & | & | \\ W_1^{\ A} & W_2^{\ A} & \overline{W}_1^{\ B} & \overline{W}_2^{\ B} \\ | & | & | & | \end{bmatrix} \begin{bmatrix} w_1 \\ w_2 \\ w_3 \\ w_4 \end{bmatrix} = {}^{E}\underset{\sim}{F}_p \tag{16}$$

where $\bar{W}_i^B = {}^A\Gamma_w W_i^B$. Nominally, from the viewpoint of actuation the system is already redundant since we now have 4 actuated d.o.f. to achieve general 3 parameter planar task wrench space. However, this combined wrench system only has rank 2 since W_1^A and W_1^B are null sets.

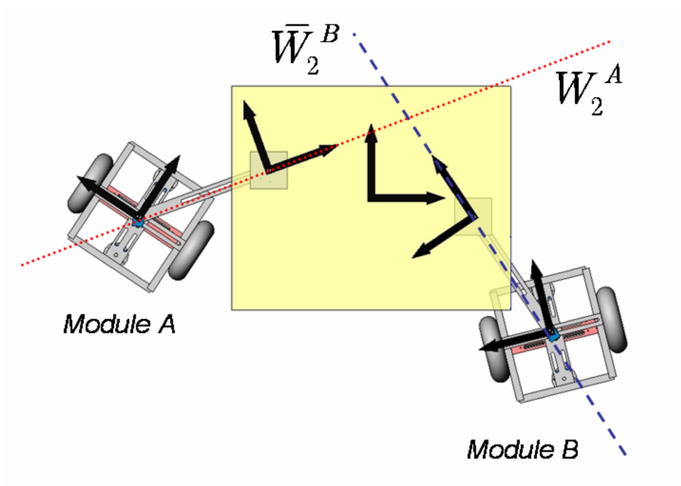

Figure 6: Lines of action of wrenches of two collaborative A-PP modules

This constitutes a force unconstrained system because there is at least one component of the force that may not be resisted (at least instantaneously). We can see that only special wrenches that lie in the span of W_2^A and $\bar{W}_2^B$ can be exactly equilibrated – all other wrenches will now be partially equilibrated by the actuation and partially resisted by the structural equilibration. Geometrically, this may be visualized as follows: the lines of actions of pure force wrenches W_2^A and $\bar{W}_2^B$ always intersect at a common point and the system is now unable to resist any pure moment applied (see Figure 6).

Case B: Cooperation between A-LP and A-PP

Additionally, since we have no control over the distribution of forces between the active and structural equilibration, this may give rise to shake and jitter. To improve the situation, one can consider an NH-RR system with first joint locked in Module A. In this case, the combined system can be written as

$$\begin{bmatrix} | & | & | & | & | \\ W_1^A & W_2^A & W_4^A & \bar{W}_1^B & \bar{W}_2^B \\ | & | & | & | & | \end{bmatrix} \begin{bmatrix} w_1 \\ w_2 \\ w_3 \\ w_4 \\ w_5 \end{bmatrix} = {}^E\underset{\sim}{F}_p \qquad (17)$$

The rank of this matrix is in general 3. We may now examine this matrix for singularity by considering the singularities of the various submatrices (10 in number). While we do not report the singularity analysis in this paper, we would like to make some general observations. We can see that the singularities can arise in an in-parallel system due to multiple reasons [30]. For example, each module can individually become singular, but this may be detected and avoided by monitoring the individual subchain Jacobian matrices. Similarly, a system level singularity may arise when multiple such modules become singular simultaneously and/or other special conditions are satisfied. This is characterized by a drop in the rank of the system wrench matrix to below 3, which is a rarer occurrence.

This is the configuration that we will employ in the experimental testing. Other alternatives may also be easily analyzed, such as: locking second joint in Module A, or locking both joints in Module A. Similarly, we may also pursue locking the corresponding joints of Module B. A listing of possible cases is given in Table 3 in Appendix A.

Experimental Setup and Evaluation

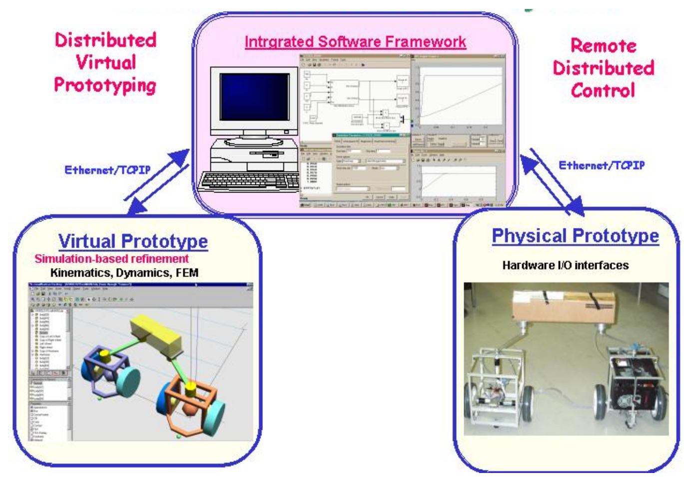

Figure 7: Paradigm for development and testing of the control scheme.

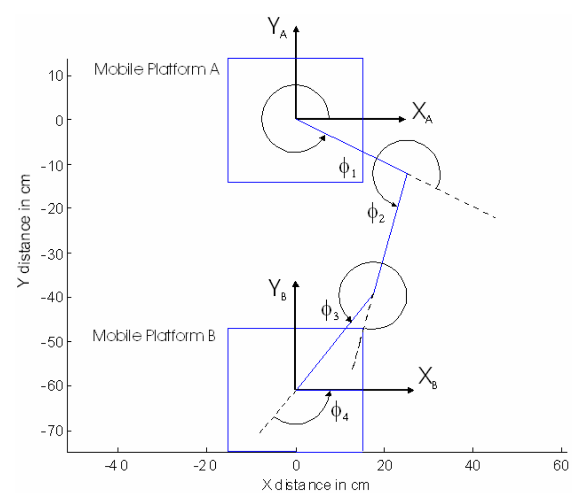

Figure 8: Initial configuration of the composite system of 2 NH-RR's.

We also examined experimental verification of cooperation in a system of 2 collaborative NH-RR's with A-LP and A-PP configurations. Our paradigm for rapid development, refinement and implementation of system design emphasizes: (i) Development of the control scheme in a user-friendly, graphical, high-level block diagrammatic language (ii) Simulation, testing and refinement of the control system by virtual prototyping; (iii) Rapid conversion of the refined control system into a form suitable for real-time execution on an embedded controller for hardware-in-the-loop testing, as shown in Figure 7. Key aspects of the design, analysis, refinement, and ultimately developing the experimental test bed for a system of two cooperating mobile manipulators are discussed in [3].

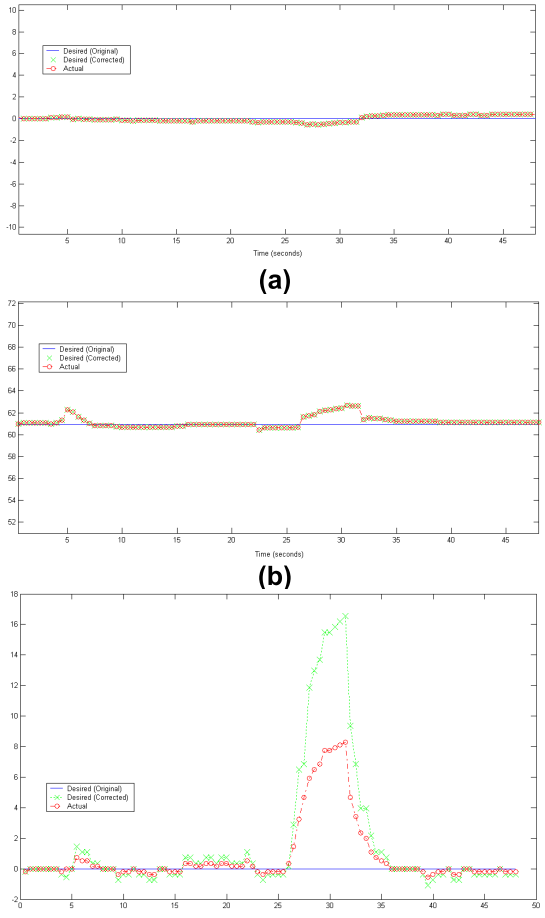

Figure 9: Articulation based estimation of frames $\{M\}$ of MP A and MP B, used for the control of MP A with respect to MP B (a) X distance (in cm), between MP A and MP B, versus Time; (b) Y distance (in cm), between MP A and MP B, versus Time; and (c) Relative Orientation (in degrees), between MP A and MP B, versus Time.

The desired task is prescribed as motion of the frame attached to the midpoint of the common object along a straight line trajectory (forward velocity of 2.54 cm/s and zero angular velocity). Figure 8 depicts the nominal desired relative configuration of the overall system with frames $\{M\}$ of Module A and Module B initially aligned in the same direction but offset by a distance of 62 cm in the Y -direction. Each NH-RR module is controlled using an online planning method described in [26]. Control is accomplished using a bilevel hierarchical scheme with an upper level design of steerable vector fields and a lower level stabilizing controller for the NH-RR type mobile manipulator. The implemented decentralized planning scheme for module uses the online measurements from the articulations in the control. The system is able to successfully transport the payload as shown in Figure 9. A video is available at [31].

A significant disturbance to the relative configuration of the system is introduced by causing the left wheels of Module A to run over a small bump. The online planning scheme is able to detect relative configuration as well as correct it to restore the desired configuration as seen in Figure 9. In each of the figures (a-c), the 'Desired (Original)' (— line) is the nominal desired trajectory that was computed offline; the 'Desired (Corrected)' (–x– line) is the desired trajectory resulting from the online sensor-based computation that deviates from the nominal desired trajectory in response to the changed relative configuration; and 'Actual' (–o– line) is the actual trajectory followed by the system as determined by post-processing the measurements of the instrumented articulations.

Note, however, that while the relative system configuration is maintained, errors relative to a global reference frame cannot be detected if both mobile bases undergo *identical simultaneous disturbances*. Detection of such absolute errors would require an external reference and is not considered here.

VI. CONCLUSION

In this paper, we examined the use of screw-theoretic analysis tools to provide a systematic framework for formulation and evaluation of system-level performance of a cooperative payload transport task by a modularly composed system of multiple wheeled mobile manipulators. Specifically, we examined the systematic modeling of the novel nonholonomic wheeled mobile manipulator modules (which form the serial-chain arms/legs); the systematic assembly of the in-parallel composite system model and subsequent analysis of the effects of selection of the actuation at the articulations (active, passive or locked) on system performance. In particular, by analyzing a 2-module composite system, we illustrated how a marginal change in the selection of actuation within the system can significantly affect the overall performance. The analysis also led to the selection of a candidate system-configuration capable of accommodating and correcting motion and force-disturbances applied at the payload which was then validated experimentally. The overall framework employed here may also be easily extended to treat larger composite system implementations with more mobile manipulator modules.

ACKNOWLEDGMENTS

We gratefully acknowledge the support from National Science Foundation CAREER Award (IIS-0347653) for this research effort.

REFERENCES

[1] Borenstein, J., Everett, B., and Feng, L., 1996, *Navigating Mobile Robots: Systems and Techniques*. A. K. Peters, Ltd., Wellesley, MA.

[2] Borenstein, J., Everett, H. R., Feng, L., and Wehe, D., 1997, "Mobile Robot Positioning: Sensors and Techniques," Special Issue on Mobile Robots, Journal of Robotic Systems, **14**, pp. 231-249.

[3] Abou-Samah, M., 2001, "A Kinematically Compatible Framework for Collaboration of Multiple Non-Holonomic Wheeled Mobile Robots," M. Eng., McGill University, Montreal, Canada.

[4] Abou-Samah, M. and Krovi, V., 2002, "Optimal Configuration Selection for a Cooperating System of Mobile Manipulators," *Proc., 2002 ASME Design Engineering Technical Conferences*, Montreal, QC, Canada.
[5] *Robot Colonies*, vol. 4(5). Kluwer Academic Publishers, Boston.
[6] Cao, Y., Fukunaga., A. S., and Kahng, A. B., 1997, "Cooperative Mobile Robotics: Antecedents and Directions," Autonomous Robots, **4**, pp. 7-27.
[7] Koivo, A. J. and Bekey, G. A., 1988, "Report of Workshop on Coordinated Multiple Robot Manipulators: Planning, Control, and Application," IEEE Transactions on Robotics and Automation, **4**, pp. 91-93.
[8] Kerr, J. and Roth, B., 1986, "Analysis of Multifingered Hands," The International Journal of Robotics Research, **4**, pp. 3-17.
[9] Salisbury, J. K. and Craig, J. J., 1982, "Articulated Hands: Force Control and Kinematic Issues," The International Journal of Robotics Research, **1**, pp. 4-17.
[10] Kumar, V. and Waldron, K. J., "Force Distribution in Closed Kinematic Chains," IEEE Transactions on Robotics and Automation, **4**, pp. 657-664.
[11] Song, S. M. and Waldron, K. J., 1989, *Machines That Walk*. MIT Press, Cambridge MA.
[12] Khatib, O., Yokoi, K., Chang, K., Ruspini, D., Holmberg, R., and Casal, A., 1996, "Vehicle/Arm Coordination and Multiple Mobile Manipulator Decentralized Cooperation," *Proc., 1996 IEEE/RSJ International Conference on Intelligent Robots and Systems*.
[13] Desai, J. and Kumar, V., 1999, "Motion Planning for Cooperating Mobile Manipulators," Journal of Robotic Systems, **10**, pp. 557-579.
[14] Tanner, H. G., Kyriakopoulos, K. J., and Krikelis, N. I., 1998, "Modeling of Multiple Mobile Manipulators Handling a Common Deformable Object," Journal of Robotic Systems, **15**, pp. 599-623.
[15] Kosuge, K., Osumi, T., Sato, M., Chiba, K., and Takeo, K., 1998, "Transportation of a Single Object by Two Decentralized-Controlled Nonholonomic Mobile Robots," *Proc., 1998 IEEE International Conference on Robotics and Automation*, Leuven, Belgium.
[16] Yamakita, M. and Suh, J.-H., 2001, "Adaptive Generation of Desired Velocity Field for Leader-Follower Type Cooperative Mobile Robots with Decentralized Pvfc," *Proc., Proc. 2001 IEEE International Conference on Robotics and Automation*.
[17] Krishnaprasad, P. S. and Tsakiris, D. P., 1995, "Oscillations Se(2)-Snakes and Motion Control," *Proc., 34th IEEE Conference on Decision and Control*, New Orleans LA.
[18] Ostrowski, J. P., 1995, "The Mechanics and Control of Undulatory Robotic Locomotion," California Institute of Technology, Pasadena CA.
[19] Campion, G., Bastin, G., and D'Andrea-Novel, B., 1996, "Structural Properties and Classification of Kinematic and Dynamic Models of Wheeled Mobile Robots," IEEE Transactions on Robotics and Automation, **12**, pp. 47-62.
[20] Pin, F. G. and Killough, M., 1994, "A New Family of Omnidirectional and Holonomic Wheeled Plaforms for Mobile Robots," IEEE Transactions on Robotics and Automation, **10**, pp. 480-489.
[21] Reister, D. B. and Unseren, M. A., 1993, "Position and Contraint Force Control of a Vehicle with Two or More Steerable Drive Wheels," IEEE Transactions on Robotics and Automation, **9**, pp. 723-731.
[22] Sreenivasan, S. V. and Waldron, K. J., 1996, "Displacement Analysis of an Actively Articulated Wheeled Vehicle Configuration with Extensions to Motion Planning on Uneven Terrain," ASME Journal of Mechanical Design, **118**, pp. 312-317.
[23] Murray, R., Li, Z., and Sastry, S., 1993, *A Mathematical Introduction to Robotic Manipulation*. CRC Press LLC, Florida.
[24] Bhatt, R. M., 2003, "Formation Motion Planning for Payload Transport by Modular Wheeled Mobile Manipulators," M.S., State University of New York at Buffalo, Buffalo.
[25] Tang, C. P., 2004, "Manipulability-Based Analysis of Cooperative Payload Transport by Robot Collectives," M.S., University at Buffalo, Buffalo NY.
[26] Tang, C. P., Bhatt, R. M., and Krovi, V., 2004, "Decentralized Kinematic Control of Payload Transport by a System of Mobile Manipulators," *Proc., Preceedings of the 2004 IEEE International Conference on Robotics and Automation*, New Orleans, LA.
[27] Bruyninckx, H. and Schutter, J. D., 1988, "Unified Kinetostatics for Serial, Parallel and Mobile Robots," *Proc., Proceedings of 6th International Symposium on Advances in Robot Kinematics*, Strobl, Austria.
[28] Waldron, K. J. and Hunt, K. H., 1991, "Series-Parallel Dualities in Actively Coordinated Mechanisms," Int. J. Robotics Research, **10**, pp. 473-480.
[29] Firmani, F. and Podhorodeski, R. P., 2004, "Force-Unconstrained Poses for a Redundantly-Actuated Planar Parallel Manipulator," Mechanism and Machine Theory, **39**, pp. 459-476.
[30] Gosselin, C. and Angeles, J., 1990, "Singularity Analysis of Closed Loop Kinematic Chains," IEEE Transactions on Robotics and Automation, **6**, pp. 281-290.
[31] Cooperative Payload Transport by Robot Collectives, 2005, available at: http://mechatronics.eng.buffalo.edu/research/mobilemanipulator/index.html.

APPENDIX A

The generation of instantaneous wrenches at individual joints does not depend on whether the actuation status of the joints (active/passive). However, it does depend on the locked status. Hence, if the nonholonomic base is always actuated, there are four possible cases that results depending on whether each of the two joint is locked or not. As seen in Table 1, the rank of the selectively non-reciprocal wrench system can vary significantly from 0 to 2. Specifically, for the case of A-PL and A-LL, there are two directions of line of action of wrench for a single joint. In such a case, the total wrench accommodated by the joint is sum of the two wrenches with same intensities equal to the intensity of that actuated joint.

Case	Instantaneous Wrenches
A-PP	$W_1 = \phi, W_2 = \begin{bmatrix} -\frac{C_2}{S_2} \\ 1 \\ -L_2 \end{bmatrix}, W_3 = \phi, W_4 = \begin{bmatrix} \frac{S_{12}}{C_{12}} \\ 1 \\ \frac{-L_1 C_1}{C_{12}} - L_2 \end{bmatrix}$
A-LP	$W_1 = \begin{bmatrix} \frac{S_{12}}{C_{12}} \\ 1 \\ -L_2 \end{bmatrix}, W_2 = \begin{bmatrix} -\frac{C_2}{S_2} \\ 1 \\ -L_2 \end{bmatrix}, W_4 = \begin{bmatrix} \frac{S_{12}}{C_{12}} \\ 1 \\ \frac{-L_1 C_1}{C_{12}} - L_2 \end{bmatrix}$
A-PL	$W_1 = W_3 = \begin{bmatrix} \frac{S_{12}}{C_{12}} \\ 1 \\ \frac{-L_1 C_1}{C_{12}} - L_2 \end{bmatrix}, W_2 = \begin{bmatrix} 1 & 0 \\ 0 & 1 \\ -L_1 S_2 & -L_1 C_2 - L_2 \end{bmatrix}$
A-LL	$W_1 = \begin{bmatrix} \frac{S_{12}}{C_{12}} & 0 \\ 1 & 0 \\ 0 & 1 \end{bmatrix}, W_2 = \begin{bmatrix} 1 & 0 \\ 0 & 1 \\ -L_1 S_2 & -L_1 C_2 - L_2 \end{bmatrix}$

Table 1: Instantaneous non-reciprocal wrench systems of an individual NH-RR with locked joints.

Case	Joints		
	NH	R	R
a	A	-	-
b	A	L	-
c	A	A	-
d	A	-	L
e	A	L	L
f	A	A	L
g	A	-	A
h	A	L	A
i	A	A	A

Table 2: Various possibilities for actuation for the individual NH-RR (A = Actuated, L = Locked).

Case	$[W]$	Rank
a	$[W]=\begin{bmatrix} -\frac{C_2}{S_2} \\ 1 \\ -L_2 \end{bmatrix}$	1
b	$[W]=\begin{bmatrix} \frac{S_{12}}{C_{12}} & -\frac{C_2}{S_2} \\ 1 & 1 \\ -L_2 & -L_2 \end{bmatrix}$	2
c	$[W]=\begin{bmatrix} -\frac{C_2}{S_2} \\ 1 \\ -L_2 \end{bmatrix}$	1
d	$[W]=\begin{bmatrix} \frac{S_{12}}{C_{12}} & 1 & 0 \\ 1 & 0 & 1 \\ \frac{-L_1C_1}{C_{12}}-L_2 & -L_1S_2 & -L_1C_2-L_2 \end{bmatrix}$	2
e	$[W]=\begin{bmatrix} \frac{S_{12}}{C_{12}} & 0 & 1 & 0 \\ 1 & 0 & 0 & 1 \\ 0 & 1 & -L_1S_2 & -L_1C_2-L_2 \end{bmatrix}$	3
f	$[W]=\begin{bmatrix} \frac{S_{12}}{C_{12}} & 1 & 0 & \frac{S_{12}}{C_{12}} \\ 1 & 0 & 1 & 1 \\ \frac{-L_1C_1}{C_{12}}-L_2 & -L_1S_2 & -L_1C_2-L_2 & \frac{-L_1C_1}{C_{12}}-L_2 \end{bmatrix}$	2
g	$[W]=\begin{bmatrix} -\frac{C_2}{S_2} & \frac{S_{12}}{C_{12}} \\ 1 & 1 \\ -L_2 & \frac{-L_1C_1}{C_{12}}-L_2 \end{bmatrix}$	2
h	$[W]=\begin{bmatrix} \frac{S_{12}}{C_{12}} & -\frac{C_2}{S_2} & \frac{S_{12}}{C_{12}} \\ 1 & 1 & 1 \\ -L_2 & -L_2 & \frac{-L_1C_1}{C_{12}}-L_2 \end{bmatrix}$	3
i	$[W]=\begin{bmatrix} -\frac{C_2}{S_2} & \frac{S_{12}}{C_{12}} \\ 1 & 1 \\ -L_2 & \frac{-L_1C_1}{C_{12}}-L_2 \end{bmatrix}$	2

Table 3: Instantaneous non-reciprocal wrench systems of an individual NH-RR with actuated and locked joints.